Experimental Section

Catalyst synthesis: W-doped Pd nanosheets were prepared by a one-pot wet-chemistry method[1]. Typically, 10 mg $Pd(acac)_2$ and 20 mg $W(CO)_6$ were dissolved into 8 mL DMF, followed by adding 2 mL acetic acid. Afterward, the mixed solution was heated to 50 °C in an oil bath and maintained for 1 h. After cooling, the black colloid was collected through centrifuging, washing with deionized water/ethanol, and drying overnight.

Characterizations: X-ray diffraction (XRD) patterns were recorded on a diffractometer (D/max-2400pc Rigaku, Japan) with Cu Kα radiation source (λ=1.54178 Å). Transmission electron microscopy (TEM) and high-resolution TEM (HRTEM) were carried out on a Tecnai G^2 F20 microscope. X-ray photoelectron spectroscopy (XPS) analysis was conducted on a PHI 5702 spectrometer. UV−vis data were recorded using a Mapada UV 6300 spectrophotometer (Shanghai, China). Gas product was detected by the gas chromatography (GC, Shimadzu GC2010).

Electrochemical measurements: Electrochemical measurements were performed with a standard three-electrode system at CHI-660E electrochemical workstation. The graphite rod, Hg/HgO and catalyst loaded on carbon paper were used as the counter electrode, reference electrode and working electrode, respectively[2-4]. The catalyst ink was prepared by ultrasonically dispersing 1 mg of catalyst in 80 μL of ethyl alcohol added with 20 μL of Nafion (5 wt%) and dried under ambient conditions. The working electrode was made by loading 20 μL of catalyst ink on carbon cloth (1×1 cm^2). All potentials reported in this work were converted to reversible hydrogen electrode (RHE) with $E_{(RHE)} = E_{(Hg/HgO)} + 0.098 + 0.0591 \times pH$, and the presented current density was normalized to geometric surface area.

Determination of NH_3: The concentration of produced NH_3 was quantitatively confirmed by an indophenol blue method[5]. Firstly, 5 g sodium salicylate and 5 g potassium sodium tartrate tetrahydrate were dissolved in 100 mL 1 M NaOH to prepare coloring agents. Afterwards, 3.5 mL NaClO was added into 100 mL deionized water to prepare oxidizing solution. Finally, 0.2 g sodium nitroprusside

dihydrate dissolved in 20 mL deionized water as catalyst solution. Briefly, 2 mL of electrolyte was removed from the electrochemical reaction vessel, followed by sequential addition of 2 mL of coloring solution, 1 mL of oxidizing solution and 0.2 mL of catalyst solution, which were mixed uniformly and then stand for 20 minutes to measure the UV-vis absorption spectrum.

NH_3 yield was calculated by

$$Y_{NH_3} = \frac{C(NH_3) \times V}{\mathrm{t} \times m_{cat}} \tag{1}$$

Faradaic efficiency (FE) was calculated by

$$FE_{NH_3} = \frac{8F \times C(NH_3) \times V}{17 \times Q} \times 100\% \tag{2}$$

where F is the Faraday constant, $C(NH_3)$ is the measured NH_3 concentration, V is the volume of the electrolyte for NH_3 collection, t is the potential applied time, m_{cat} is the mass loading of catalyst on carbon cloth and Q is the quantity of applied electricity.

Determination of NO_2^-: The NO_2^- in liquid products were detected according to the method of Griess method[6]. In the Griess method, the coloring agents were prepared by dissolving H_3PO_4 (2.94 mL), N-(1-naphthyl) ethyldiamine dihydrochloride (0.1 g), and sulfonamide (1.0 g) in deionized H_2O (50 mL). Adding 0.1 mL diluted electrolyte with distilled water in the typical process, and the mixed solution was allowed to stand at room temperature for 10-20 min to generate a magenta azodye. Finally, the concentration of NO_2^- was determined by the peak at 540 nm on UV-Vis Spectroscopy.

NO_2^- yield was calculated by：

$$Y_{NO_2^-} = \frac{C\ (NO_2^-) \times V}{\mathrm{t} \times m_{cat}} \tag{3}$$

Faradaic efficiency (FE) was calculated by：

$$FE_{NO_2^-} = \frac{2F \times C(NO_2^-) \times V}{46 \times Q} \times 100\% \tag{4}$$

where F is the Faraday constant, $C(NO_2^-)$ is the measured NO_2^- concentration, V is the volume of the electrolyte for NO_2^- collection, t is the potential applied time, m_{cat} is the

mass loading of catalyst on CP and Q is the quantity of applied electricity.

Determination of N_2H_4: The concentration of N_2H_4 was determined by Watt and Chrisp method[7]. A mixture of $C_9H_{11}NO$ (5.99 g), HCl (30 mL), and C_2H_5OH (300 mL) was used as a chromogenic reagent. Typically, 1 mL electrolyte was added into 1 mL prepared chromogenic reagent and stirred for 15 min in the dark. The absorbance at 455 nm was measured to quantify the N_2H_4 concentration with a standard curve of hydrazine.

Calculation details: Spin-polarized plane-wave density functional theory (DFT) calculations were carried out using a Cambridge sequential total energy package (CASTEP) program[9]. Perdew−Burke−Ernzerh (PBE) of generalized gradient approximation (GGA) was employed to describe the exchange-correlation potential with considering the van der Waals (vdW) interactions by a DFT-D method. To ensure the convergence for the total energy, we adopted a plane-wave cutoff energy of 350 eV with a Monkhorst-Pack grid (1×1×1) for k-point sampling. Besides, the convergence of energy and forces was set to be 1.0×10^{-5} eV/atom and 0.01 eV/Å, respectively. The NO_3 reduction reaction on different catalysts surfaces were simulated according to the following reactions[10]:

$$*NO_3 + H_2O + 2e^- \rightarrow *NO_2 + 2OH^- \quad (5a)$$

$$*NO_2 + H_2O + 2e^- \rightarrow *NO + 2OH^- \quad (5b)$$

$$*NO + H_2O + 2e^- \rightarrow *N + 2OH^- \quad (5c)$$

$$*N + H_2O + e^- \rightarrow *NH + OH^- \quad (5d)$$

$$*NH + H_2O + e^- \rightarrow *NH_2 + OH^- \quad (5e)$$

$$*NH_2 + H_2O + e^- \rightarrow *NH_3 + OH^- \quad (5g)$$

where the * represent the adsorption site. The Gibbs free energy change (ΔG，298 K) of each step was calculated by the following equation[11]:

$$\Delta G = \Delta E + \Delta E_{ZPE} - T\Delta S \quad (6)$$

where ΔE is the adsorption energy, ΔZPE is the zero point energy difference and $T\Delta S$ is the entropy difference between the gas phase and adsorbed state.

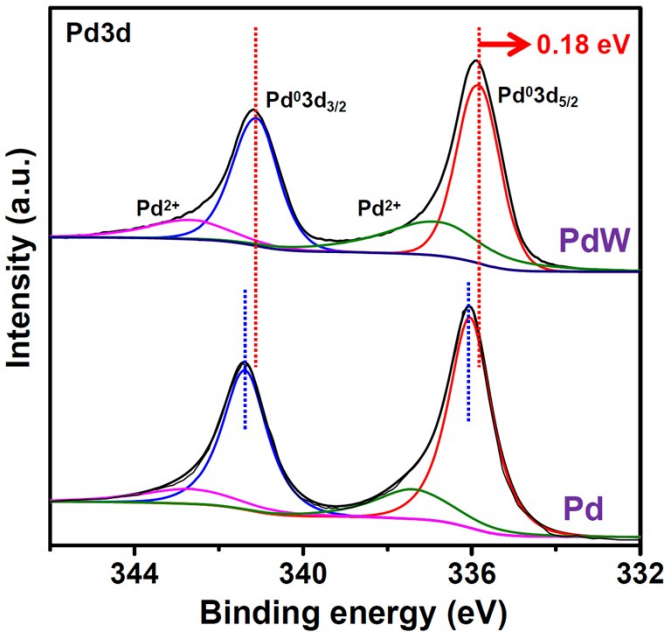

Fig. S1. Pd3d spectra of Pd and PdW.

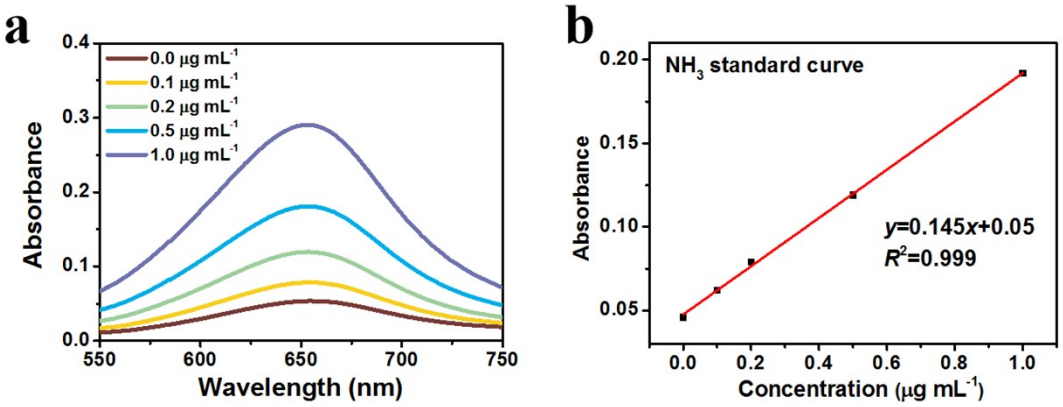

Fig. S2. (a) UV-vis absorption spectra and corresponding (b) calibration curve used for calculation of NH_3 concentrations.

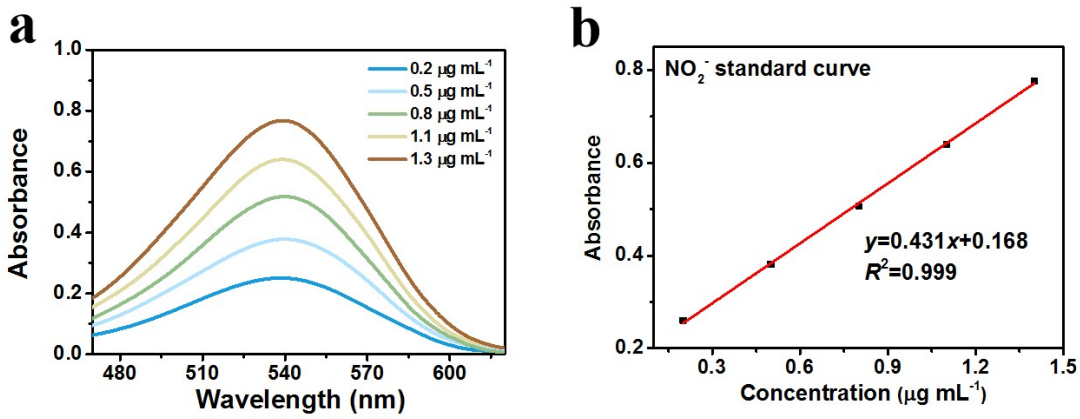

Fig. S3. (a) UV-vis absorption spectra and corresponding (b) calibration curve used for calculation of NO_2^- concentrations.

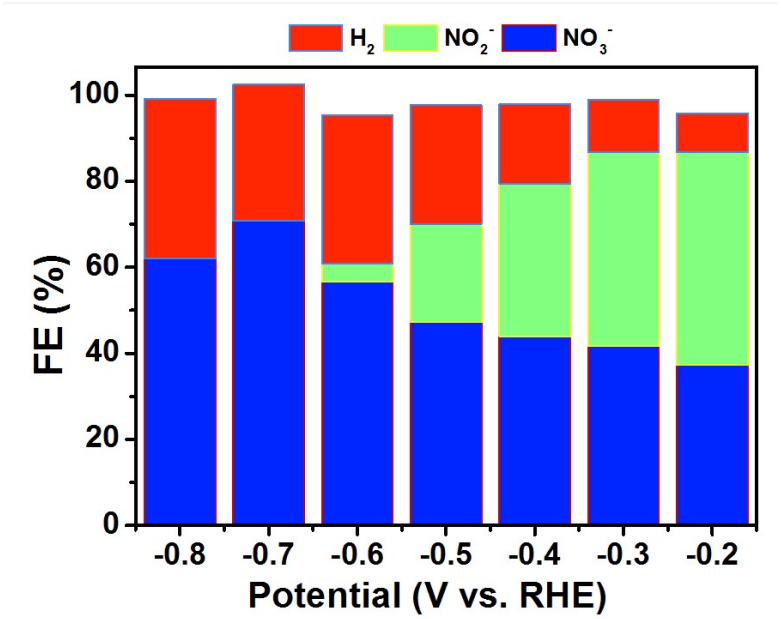

Fig. S4. Selectivity for various products over PdW after 1 h of NO_3RR electrolysis at various potentials.

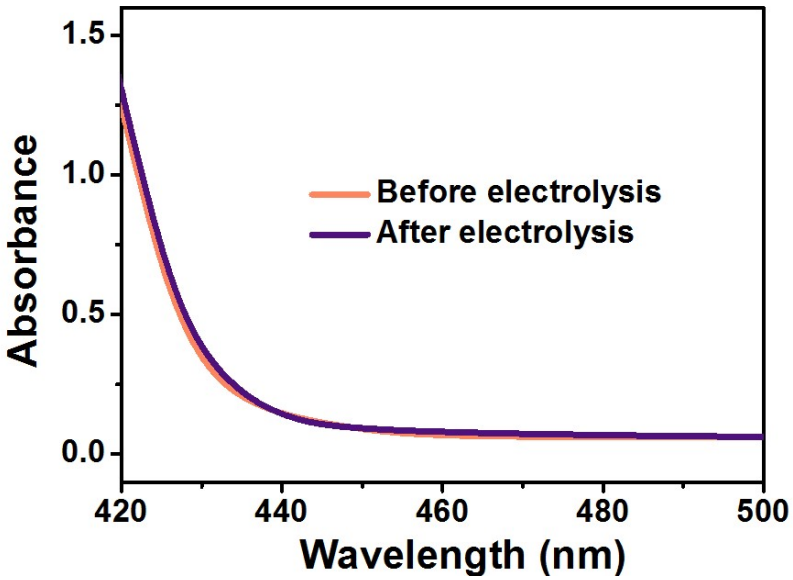

Fig. S5. UV-vis spectra of the electrolytes (stained with the chemical indicator based on the method of Watt and Chrisp) before and after 1 h of NO_3RR electrolysis on PdW at -0.7 V.

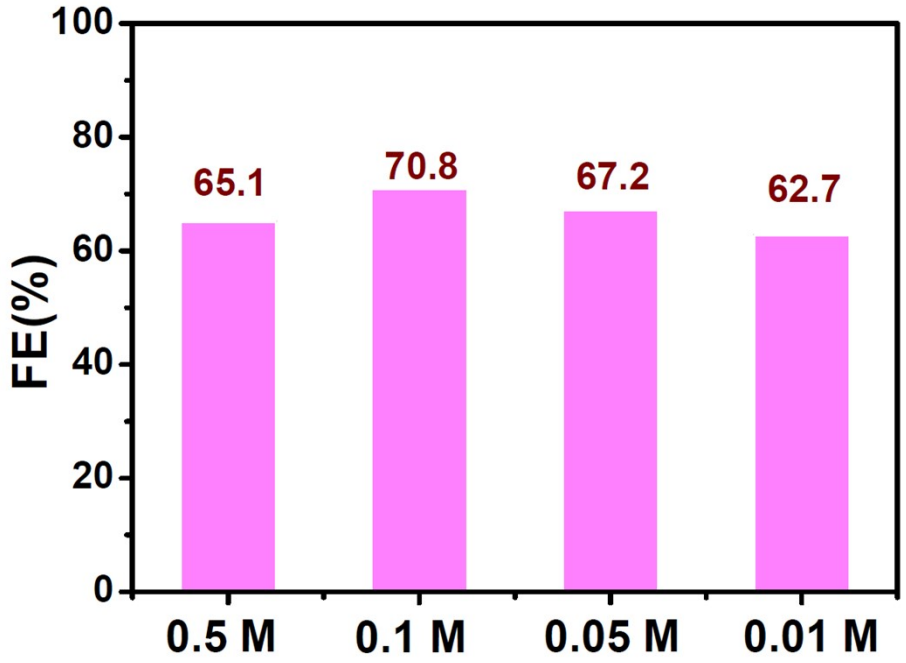

Fig. S6. FE of PdW at different starting $NaNO_3$ concentrations at -0.7 V.

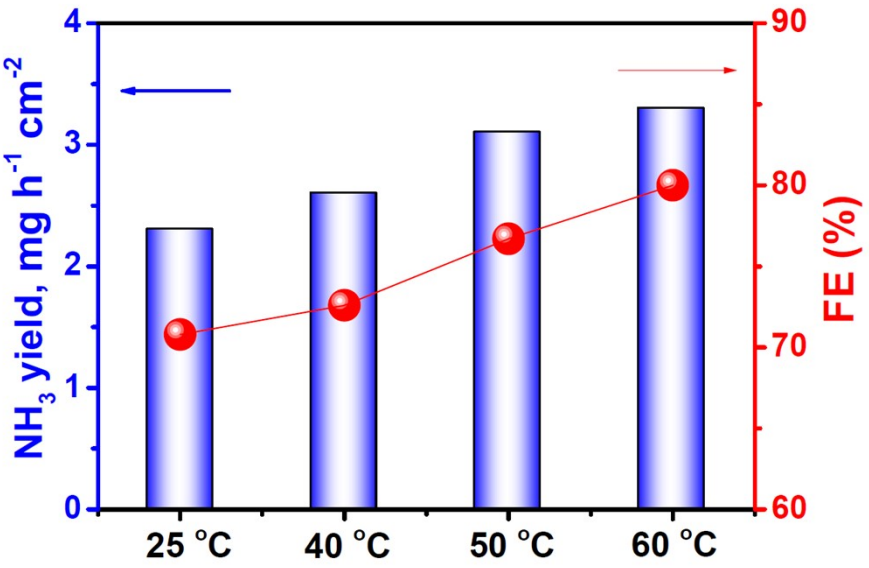

Fig. S7. NH_3 yields and FEs of PdW at different temperatures under the potential of -0.7 V.

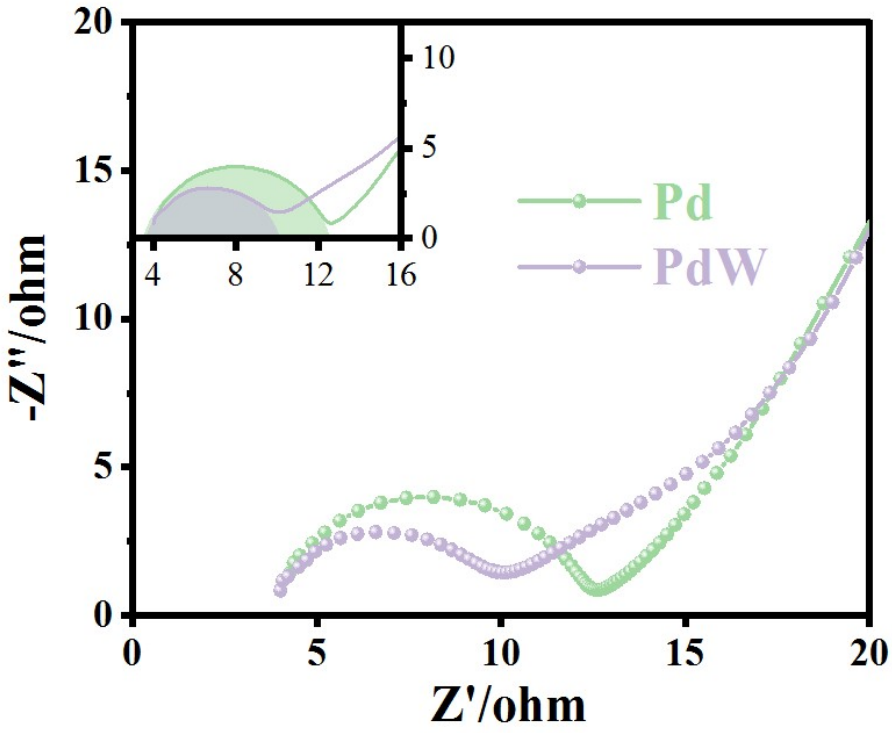

Fig. S8. Electrochemical impendence spectra of Pd and PdW.

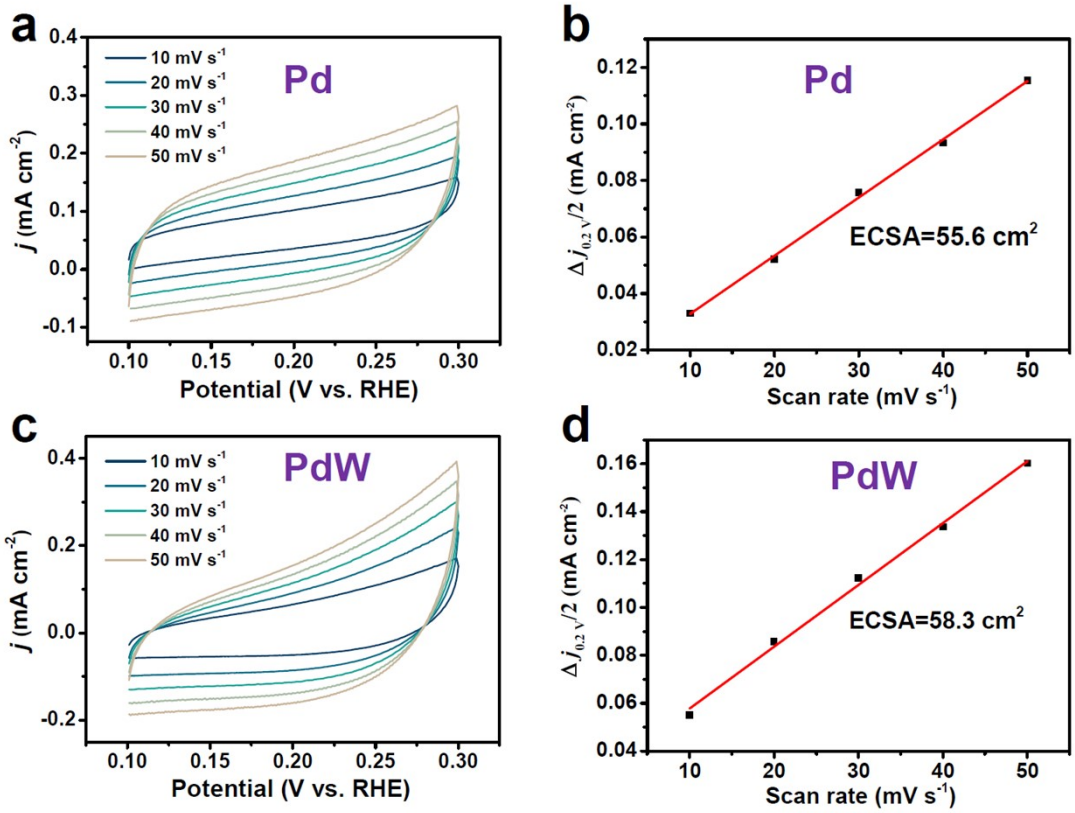

Fig. S9. Calculated electrochemical active specific areas (ECSA) of Pd (a, b) and PdW (c, d).

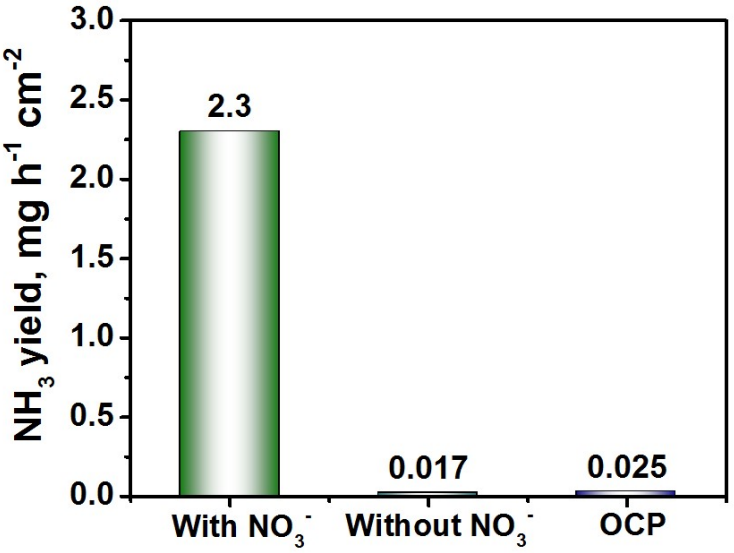

Fig. S10. NH_3 yields of PdW at three different conditions: with NO_3^-, without NO_3^- and at open circuit potential (OCP).

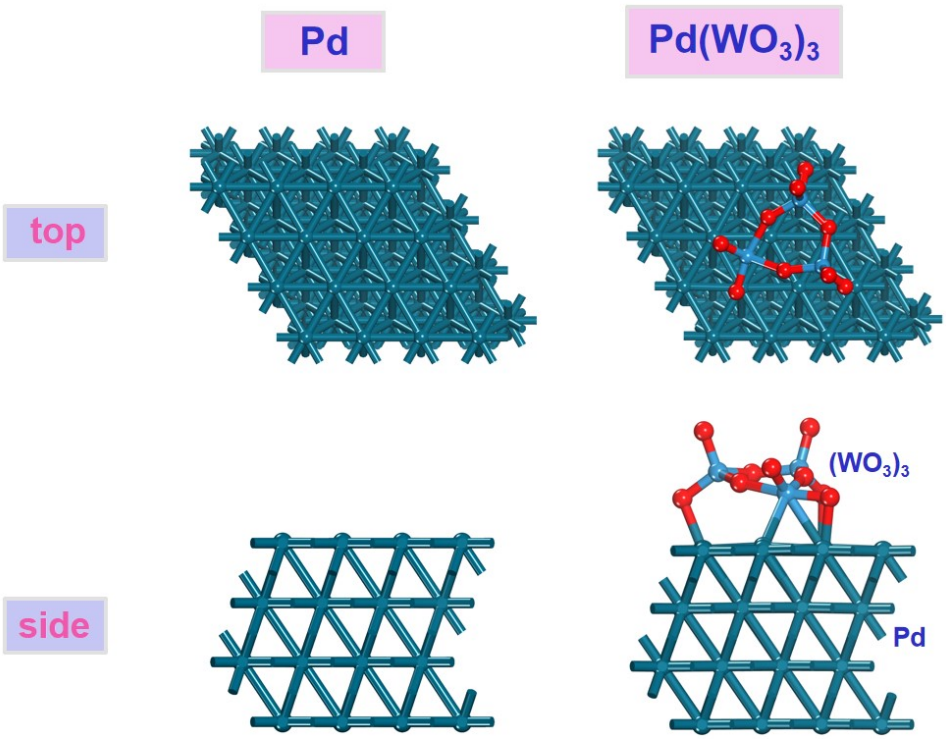

Fig. S11. The atomic structures of Pd and $Pd(WO_3)_3$.

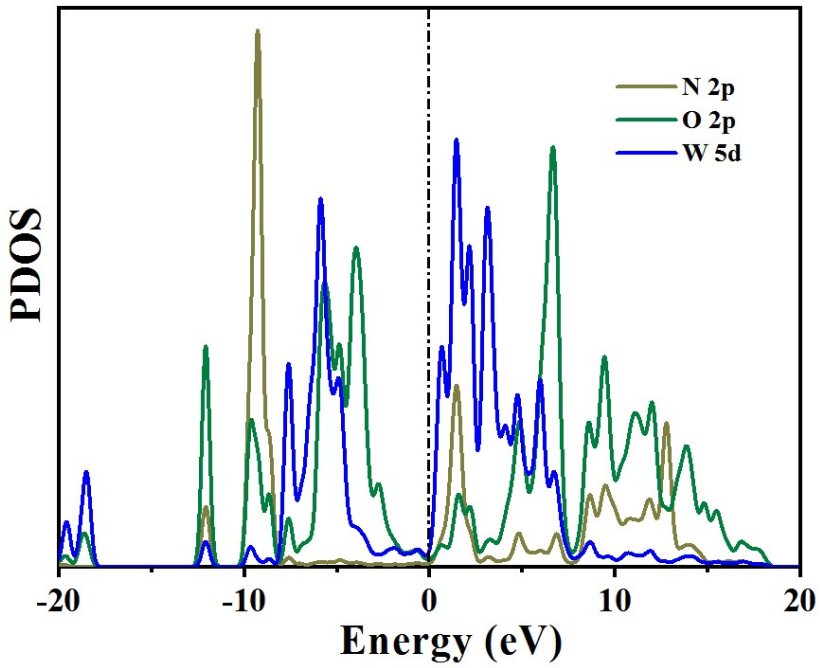

Fig. S12. PDOS analysis for N-2p, O -2p and W-5d orbitals after NO_3^- adsorption on PdW.

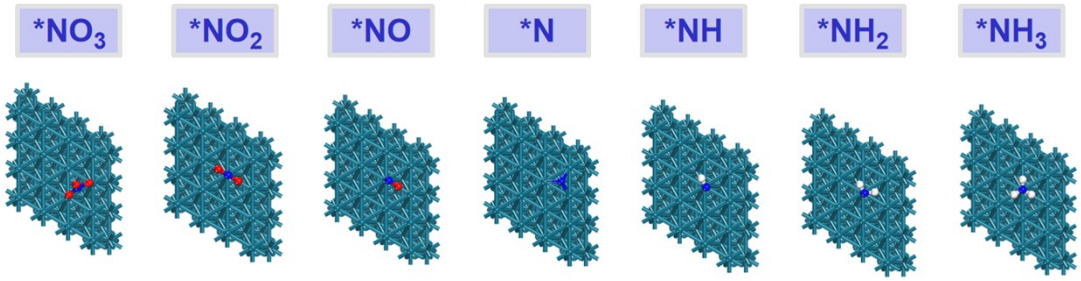

Fig. S13. Atomic structures of the NO_3RR reaction intermediates on Pd.

Table S1. Comparison of optimum NH_3 yield and Faradic efficiency (FE) for recently reported state-of-the-art NO_3RR electrocatalysts at ambient conditions

Catalyst	Electrolyte	NH_3 yield rate @ Optimum Potential (V vs RHE)	FE @ Optimum Potential (V vs RHE)	Long-term Stability	Ref.
Fe_3O_4/SS	0.1 M NaOH (0.1 M $NaNO_3$)	10.145 mg·h^{-1}·cm^{-2}@-0.5	91.5% @-0.5	12 h	Nano Res., 2022, 15(4): 3050-3055
TiO_{2-x}	0.5 M Na_2SO_4（50 ppm NO_3^-）	7.650 mg·h^{-1} mg^{-1}@-0.6	85% @-0.6	/	ACS Catal. 2020, 10, 6, 3533–3540
Cu–PTCDA	1 M PBS（500 ppm KNO_3）	436 ± 85 μg h^{-1} cm^{-2}@-0.4	85.9% @-0.4	15 h	Nat. Energy, 2020, 5(8): 605-613
Fe SAC	0.25 M K_2SO_4（0.50 M KNO_3）	0.46 mM h^{-1} cm^{-2} @-0.85	75% @-0.66	15 h	Nat. Commun., 2021, 12(1): 1-10
CuCl_BEF	0.5 M Na_2SO_4（100 mg/LNO_3^-）	1.82 mg h^{-1} cm^{-2}@-1.0	44.7% @-1.0	15 h	Angew. Chem., Int. Ed., 2021, 60(42): 22933-22939
RuNi-MOF	0.1 M Na_2SO_4（50 mg L^{-1} NO_3^-）	274 μg h^{-1} mg^{-1}@-1.7	73% @-1.2	/	J. Mater. Chem. A, 2022,10, 3963-3969
$Cu_{28}Pd_{72}$	50 mM Na_2SO_4 (22.5 mgL^{-1}NO_3^-)	/	28.7% @-0.8	10 h	Chem. Eng. J., 2022, 435: 134969
Pd NDs/Zr-MOF	0.1 M Na_2SO_4 (500 ppm NO_3^-)	287.31mM·h^{-1}·g^{-1} @-1.3	58.1% @-1.3	6 h	Nano Lett. 2022, 22, 6, 2529–2537
This work	**0.5 M Na_2SO_4（0.1 M NO_3^-）**	**2.3 mg h^{-1} cm^{-2} (11.5 mg h^{-1} mg^{-1}) @-0.7 V**	**70.8% @-0.7**	**12 h**	**This Work**

REFERENCE

1. H. Yu, T. Zhou, Z. Wang, Y. Xu, X. Li, L. Wang and H. Wang, *Angew. Chem. Int. Ed.*, 2021, **133**, 12134-12138.
2. K. Chu, W. Gu, Q. Li, Y. Liu, Y. Tian and W. J. J. o. E. C. Liu, *J. Energy Chem.*, 2021, **53**, 82-89.
3. K. Chu, Y. P. Liu, Y. B. Li, Y. L. Guo, Y. Tian and H. Zhang, *Appl. Catal., B*, 2020, **264**, 118525.
4. Z. Fang, Z. Jin, S. Tang, P. Li, P. Wu and G. Yu, *ACS Nano*, 2021, **16**, 1072–1081.
5. D. Zhu, L. Zhang, R. E. Ruther and R. J. J. N. m. Hamers, *Nat. Mater.*, 2013, **12**, 836-841.
6. L. C. Green, D. A. Wagner, J. Glogowski, P. L. Skipper, J. S. Wishnok and S. R. Tannenbaum, *Anal. Biochem.*, 1982, **126**, 131-138.
7. G. W. Watt and J. D. J. A. C. Chrisp, *Anal. Chem.*, 1952, **24**, 2006-2008.
8. J. Qin, K. Wu, L. Chen, X. Wang, Q. Zhao, B. Liu and Z. J. J. o. M. C. A. Ye, *J. Mater. Chem. A*, 2022, **10**, 3963-3969.
9. S. J. Clark, M. D. Segall, C. J. Pickard, P. J. Hasnip, M. I. J. Probert, K. Refson and M. C. Payne, *Z. Kristallogr. - Cryst. Mater.*, 2005, **220**, 567-570.
10. Y. Wang, A. Xu, Z. Wang, L. Huang, J. Li, F. Li, J. Wicks, M. Luo, D.-H. Nam, C.-S. Tan, Y. Ding, J. Wu, Y. Lum, C.-T. Dinh, D. Sinton, G. Zheng and E. H. Sargent, *J. Am. Chem. Soc.*, 2020, **142**, 5702-5708.
11. A. A. Peterson, F. Abild-Pedersen, F. Studt, J. Rossmeisl, J. K. J. E. Nørskov and E. Science, 2010, **3**, 1311-1315.